HIGH RESOLUTION CROP MAPPING ALONG THE GROWING SEASON: METHODOLOGICAL DEVELOPMENTS TOWARDS AN OPERATIONAL EXPLOITATION OF SENTINEL-1, 2 AND 3

François Waldner, Raphaël d'Andrimont, and Pierre Defourny

Université catholique de Louvain, Earth and Life Institute - Environmental Sciences, Croix du Sud 2, 1348 Louvain-La-Neuve, Belgium,
{francois.waldner; raphael.dandrimont; pierre.defourny}@uclouvain.be

ABSTRACT

Agricultural remote sensing can be used operationally to tackle the issues of food security and speculation on food commodities. Timely and reliable crop specific maps are essential to production forecasting because it supports the estimation of its two components: yield and planted area. This study proposes some developments towards an operational exploitation of Sentinel-1,2 and 3 for crop classification along the season. Using proxy data, the method is demonstrated over a large site in Russia. Three maps are produced along the season with an increasing accuracy and an increasing number of class: cropland in September, crop group in March and crop species from April to August.

Key words: agriculture; crop mapping; multi-sensor; multi-scale; along the season.

1. INTRODUCTION

In a context of increasing pressures on croplands, the G20 has recognized the importance of timely, accurate and transparent information to address food price volatility and quality of data on agricultural market. Production forecasting implies both yield and planted area estimation. Reliable crop maps are often a prerequisite as they support direct area estimates and improve the retrieval of the biophysical variables needed in the growth models[1].

Crop discrimination is made possible by the differential phenological development of crops. Maximum discrimination between different crops occurs at different stages in the growth cycle and sometimes imperceptible with a single image [2]. Crop mapping has already been extensively studied using time-series of moderate spatial resolution images [3], high resolution images [4], Synthetic Aperture Radar (SAR) data [5], a combination of SAR and high resolution [6] or high and moderate resolution [7]. A useful crop mask is one that captures the salient features of the current growing season with a certain level of accuracy [8] – De Wit and Clevers [9] suggested an accuracy target of 85%. Crop masks should be available as early in the season as possible, even with less accuracy than end-of-season estimates [10], so that decision-makers have time to respond to the likely impacts of the forecast. But to date most experiments looked at it from an end of season point of view, selecting the best-suited band/date combination to maximize the classification accuracy. Early mapping along the the growing season represent a major challenge as only incomplete growing season time-series information is available [8]. In such a context, reducing dependence on one sensor would support operational crop monitoring as sensor malfunction and cloud coverage at critical periods might jeopardize the accuracy requirements of the map[11].

To answer the need for accurate and timely crop maps, this articles proposes some developments towards an operational exploitation of Sentinel-1, 2 and 3 to produce high resolution crop specific maps updated along the growing season. The overarching objective aims at developing a classification method that combines the advantages of each satellite: the temporal coverage of Sentinel-3, the high resolution of Sentinel-2 and the weather independent acquisitions of Sentinel-1. The method integrates time-series and object-based analysis as well as data mining techniques and is demonstrated over a large site in Russia. The methodological development targets three successive outputs:

1. At the beginning of cropping season, a *pre-seasonal cropland* extent map is produced using a dedicated land cover algorithm based on the previous year metrics at moderate resolution. The best local land cover map available helps this early diagnosis.
2. At the end of the winter, a *crop group* recognition map distinguishing winter and summer crops is delivered thanks to a phenological object-based time-series classification of medium resolution data.
3. Along the growing season, a multi-sensor *crop specific* classification is finally achieved and updated as data acquisition progresses taking into account the

Proc. 'ESA Living Planet Symposium 2013', Edinburgh, UK
9–13 September 2013 (ESA SP-722, December 2013)

agricultural calendar and the crop rotation systems. Through an iterative segmentation and classification scheme, moderate and high resolution optical images and radar data at each new acquisition of high resolution imagery.

All over the season, this combination of three sensors will thus allow a continuous monitoring at regional scale. In this way, crop maps will be updated along the season with an increased precision (increased number of classes and decreased omission and commission errors) that, in chain, will support the retrieval of bio-physical variables for crop growth models and early acreage estimation. The first section of this paper presents the study site as well as the data used and their pre-processing. The second section details the methodology of the three products and the results are discussed in the third section.

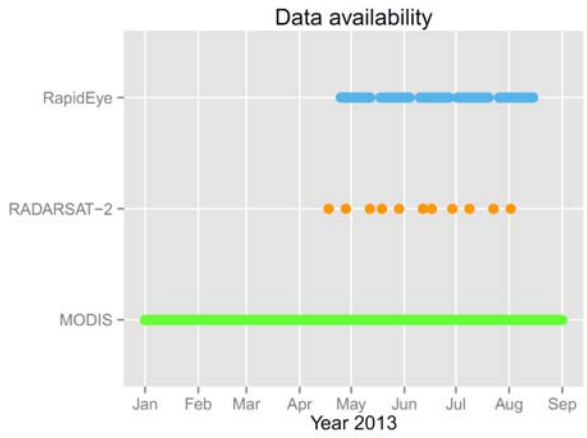

Figure 1. Data acquisition plan. It includes five coverages with RapidEye, 11 with RapidEye. MODIS data were acquired all from January 2012 to September 2013.

2. MATERIAL

2.1. Study area and field data

The study focuses on the Russian oblast of Tula (25,700 km^2), an important winter wheat growing area (about 270 000 ha). The average field size is 70-ha. Its geographic proximity to Moscow allows easy field data collection. Reference samples for training and validation were collected in July 2013 by the Russian Agro-Meteorological Institute (AMI). The data set contains 600 observations of 19 different agricultural classes (spring barley, buckwheat, cabbage, chamomile, carrot, clover, fallow land, lucerne, maize, millet, oats, pea, potato, rapeseed, winter rye, sugar beet, sunflower, spring wheat, winter wheat) largely dominated by winter wheat and spring barley. A parcel database is also available. Fields were manually digitized on Landsat-5 and 7 images and last updated in 2012.

2.2. Satellite data and pre-processing

For the growing season of 2013, Sentinel data was simulated by similar and currently available satellites (see Tab.1 for a comparison). Eleven Radarsat-2 images and 5 RapidEye coverage were acquired from February to August (Fig.1). MODIS acquisitions span from January 2012 to August 2013.

Instead of Sentinel-1 images, 11 Radarsat-2 ScanSar Narrow images were acquired in dual polarization VV-VH. According to the literature vertical polarization seems the most adequate polarization for C-band crop recognition [9, 11]. Images were multi-looked, ortho-rectified, radiometrically calibrated and co-registered. A 9x9 enhanced Frost filter reduced the speckle.

RapidEye data served as proxy for Sentinel-2. Five coverages of Tula were ordered. Each coverage totals about 110 tiles of 25x25 km. The images were ortho-rectified and converted to top of atmosphere reflectance. The unusable data mask provided along with the data, even though perfectible, masked out clouds. To achieve a full coverage of the oblast meeting a certain threshold of cloud contamination, 18-20 days acquisition time windows were defined. Even with such a long period and multiple acquisition attempts, some images could not meet the cloud coverage requirements. This emphasize the pertinence of multi-sensor combination.

MODIS data simulated Sentinel-3. From daily quality controlled reflectance values, 10-day mean composites were produced according to the procedure developed by [12]. The mean compositing reduces bidirectional reflectance distribution function and atmospheric artifacts, produces spatially homogeneous cloud-masked composites with good radiometric consistency and does not requiring model adjustment or additional parametrization. Because field survey revealed strong variations in soil color, a soil adjusted vegetation index with a self-adjusting soil brightness correction factor, the MSAVI$_2$ [13], was calculated for for every pixel of the image. Thus, the MSAVI$_2$ minimizes soil background influences and increases the dynamic range of the vegetation sensitivity. It is calculated as follows:

$$\text{MSAVI}_2 = \frac{2\rho_{nir} + 1 - \sqrt{(2\rho_{nir}+1)^2 - 8(\rho_{nir} - \rho_{red})}}{2} \quad (1)$$

where ρ_{nir} and ρ_{red} are reflectances in the near infrared and red band, respectively. Time-series were then smoothed with the Whittaker filter [14]. The gap filling ability of this filter is particularly interesting because of the persistent cloud coverage in the area.

Table 1. Comparison of Sentinel-1,2 and 3 with their respective proxy. Only the spectral bands used in this study area are detailed.

	SENTINEL-1	RADARSAT-2	SENTINEL-2	RAPIDEYE	SENTINEL-3	MODIS
Nominal Swath	80-km	300-km	290-km	77-km	1250-km	2330-km
Wavelength (μm)/frequency	C-band	C-band	blue (0.42-0.55), green (0.53-0.59), red (0.63-0.69), red-edge (0.69-0.72, 0.72-0.75, 0.76-0.8, 0.84-0.89), near-infrared (0.72-0.96) and 5 others	blue (0.40-0.51), green (0.52-0.59), red(0.63-0.685), red-edge (0.69-0.73), near-infrared (0.76-0.85)	red (0.6-0.7) , near-infrared (0.88-0.89) and 19 others	red (0.62-0.67), near-infrared (0.84-0.88) and 34 others
Polarization	HH+HV VV+VH	HH+HV VV+VH	NA	NA	NA	NA
Beam Incidence angle	20°-41°	20°-46°	NA	NA	NA	NA
Ground resolution	5-m	25-m	10-m	5-m	300-m	250-m
Repeat cycle	2 days using a constellation of satellites	programmable	5 days with a pair	daily with 5 satellites	1-2days with a pair	1-2 days

3. METHODOLOGY

Combining the proxies, three maps will be produced along the season taking advantage of the accumulation of the information along the growing season to progressively further discriminate the different crop species. Such multi-scale and multi-spectral information should improve the temporal density of observations essential to capture the crops phenology, which is the main criterion of the discrimination process. The joint use of high spatial resolution of both optical and radar images is expected to resolved most field. The method targets the production of three products – a pre-seasonal cropland map, a crop group map and a crop specific map – released in September and March for the two first and updated from April to August for the latter.

3.1. Pre-seasonal cropland layer

Understanding the area and extent of croplands as well as its evolution is important for a variety of societal and environmental reasons [15]. Studies have first discarded non-agricultural areas by means of fieldwork and photo-interpretation [16], masks of non-arable land from land cover maps [17] or farmland parcels delineation[9]. Using the best available land cover information seems the most transposable solution to other sites but not necessarily the most accurate. Indeed, most of the available land cover maps do not target agricultural land and need adjustments to fit the local conditions. Plus, changes may have occurred since their production.

Iterative trimming is a change detection technique that identifies outliers as plausible candidates for change [18]. Radoux et al. [19] applied non-parametric iterative trimming to automate image-to-map discrepancy detection. However, non-parametric is computationnaly itensive and processing time increases exponentially with the dimensionality. This study proposes a multivariate normal iterative trimming alternative because the normal hypothesis reduces considerably the processing time. For each class, the selection of outliers relied on a probability threshold α which specifies the limit at which an observation is considered an outlier. The distribution is iteratively trimmed until no more outliers are identified. For the normal case, it gives:

$$(x-\mu)'\Sigma^{-1}(x-\mu) \leq \chi^2_p(\alpha) \quad (2)$$

where χ^2 is the upper (100α)th percentile of a χ^2 distribution with p degrees of freedom.

At the beginning of the season (September in Russia), cropland at year t is mapped with the annual time-series of year $t-1$. According to the Hughes phenomenon,

images carrying little discriminating information may decrease the classification accuracy. To reduce the dimensionality, four metrics were extracted from the time-series because of their ability in separating cropland from other land covers: the sum, the mean, the range and the norm of the pixels' signal.

Multivariate normal iterative trimming was applied on each class of the GlobCover map but the agricultural mosaic classes. These classes and the resulting outliers were reclassified according to the maximum likelihood decision rule. A priori probabilities were computed from the initial land cover map with mixed classes probabilities redistributed. The four metrics were standardized to avoid confusion between different units. The new land cover map details six classes: rainfed cropland, urban, water and three classes of forest. Non-crop classes were finally grouped in order to focus the classification on crop detection. Accuracy was evaluated by means of the Pareto boundary method [20].

3.2. Crop Group layer

With its continental climate, the Tula region has two very distinctive planting period: august for winter crops and March-April for summer crop. Winter wheat is generally sown in mid-August and grows until the tillers prior to the dormancy period that generally begins in December. After the winter dormancy, it resumes growth late in March (Fig 2). Sensors with high temporal repetitiveness such as MODIS and Sentinel-3 allow to make rapid updates of winter-wheat planted area, with the ability to recognize a considerable part of the planted area already before winter.

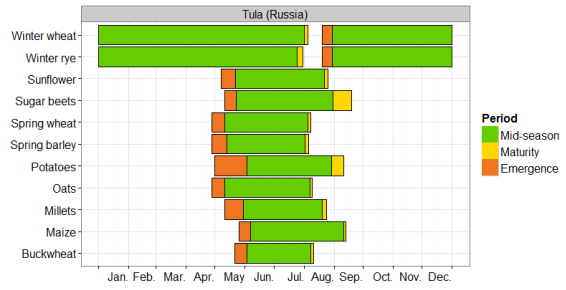

Figure 2. Crop calendar for the Tula region. The calendar illustrates the timing differences of the development stages of the main crops.

A two-step phenological object-based classification addresses the binary classification of winter crops versus summer crops. In the first step, objects are derived by means of a segmentation on the harmonic components of the time-series. In the second, an automated time-series analysis based on phenological metrics classifies the objects in the two classes. The previously derived cropland masks out the non-agricultural areas.

Fourier or harmonic analysis transforms an input signal from the time domain into the frequency domain. The resulting harmonic components summarize information on the signal: they capture the temporal dynamics while it reduces the dimension and the noise while preserving phenological characteristics [21]. Performing an analysis on the frequency components, a distinction can be made between signals frequency terms relates to vegetation dynamics [22].

In a closed interval [0;N], each continuous and periodic signal can be decomposed into a series of sine-waves with increasing frequencies and an additive term that together reconstruct the initial signal:

$$f(x) = \frac{a_0}{2} + \sum_{i=1}^{i=N/2} a_i \cos(\frac{2\pi i x}{N} - \phi_i) \qquad (3)$$

The Fourier transform is a function that transform a time series and returns a complex array with a real (a) and an imaginary (b) part that can be converted to polar form. Each order i is defined by a phase ϕ_i and an amplitude a_i:

$$a_i = \sqrt{a_i^2 + b_i^2} \qquad (4)$$

$$\phi_i = \arctan \frac{b_i}{a_i} \qquad (5)$$

The high orders contain mainly noise.

Land cover and crops exhibit distinctive temporal patterns and thus are characterized by different phase and amplitude parameters. Harmonic analysis was applied pixel-wise. Similar pixels were then spatially grouped based on the similarity of the two first harmonic and the additive term using the multi-resolution segmentation algorithm. Multi-date segmentation is known to perform better than single-date but requires the prior identification of key-dates. Segmenting on the harmonic components is an alternative to overcome this constraint.

A simple rule-based classification was developed based on the major characteristics of winter crop time-series: the winter growth. For every image from the 150th day of sowing year to the 90th day of harvesting year, vegetation index values were averaged per objects. The spatial aggregation of the surface reflectance at object level reinforces its signal to noise ratio.

To ensure year-to-year robustness, it is necessary to consider the phenological calendar rather than the Julian day. The automated adaptive recognition decision rule relies on the presence or absence of an observable winter growth peak, i.e. a maximum (Fig. 3). According to the specificity of the task (i.e. partial time-series), new metrics have to be defined: (i) the snow date corresponds to the dekade during which the MSAVI signal falls below a threshold, (ii) the maximum of vegetation is the local

maximum MSAVI value at the winter growth peak and (iii) the local minimum preceding the winter peak.

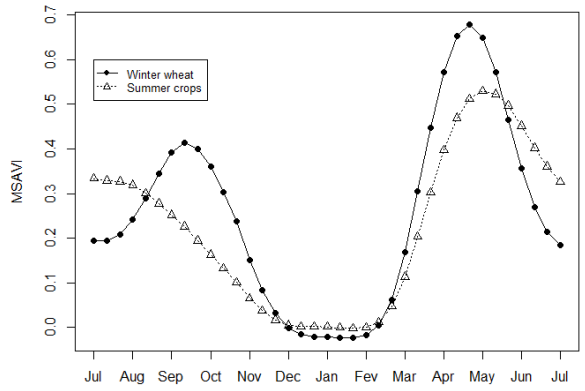

Figure 3. Typical temporal profile of winter wheat and summer crops. The profiles are consistent with the crop calendar: winter wheat exhibits a winter growth starting in August. Snow covers both winter and summer crop fields from December to March and makes them inseparable.

The simplest decision rule would classify as winter crop every feature with a winter peak, but this hypothesis does not hold as other landscape elements also exhibit a maximum. Usually, those elements however are characterized by a rapid drop and then increase of the signal whereas winter crop shows a plateau corresponding to field preparation and sowing. To tighten the rule, the minimum and the maximum are converted into local average of the metric values: an object is classified as winter crop if $mean(max) > mean(min)$. This filters out objects without a significant increase in their respective trajectory.

To strengthen the accuracy of the classification, a cross-validation based on the harmonic components is added. The 25 nearest (in Euclidean distance) vectors are found and the final label is decided by majority vote. The harmonic component values were first standardized and then averaged per object. In-situ validation data were reduced to a binary legend that separates winter wheat from any other crop. Accuracy was assessed with the traditional error matrix and its derived statistics.

3.3. Crop specific layer

For the crop specific layer, the goal is to deliver a crop specific mask along the season updated at each acquisition of high resolution either radar or optical. This translates into an iterative classification scheme: at each acquisition, the newest image is segmented using the multi-resolution algorithm [23]. This single-date classification is constrained by the former to make use of multi-temporal information. Objects mean reflectances and back-scattering coefficients are extracted for each objects of the available time-series. MODIS time-series is smoothed and gap-filled with the Whittaker smoother. Objects with missing values were regarded as a population and new values were imputed according to an inverse distance weighted mean of the 3 nearest neighbors.

This study investigates the potentiality of the random forest classifier to accurately discriminate crops [24]. Random forests are particularly interesting as they are insensitive to noise or overtraining, and are also capable of handling unbalanced data sets. Its internal selection of variables is expected to prevent side-effects of high dimensionality as information accumulates. At each new acquisition, a classifier with 500 trees was trained taking into account all the information available at that time.

For this paper, the method was tested on a subset of the region encompassing six RapidEye tiles (about 3600 km^2). As a result, the in-situ data set available for training and validation was reduced in terms classes and less populated. This reduction might affect the quality of the training and the accuracy of the map. The nine remaining classes to classify were bare soil, urban areas, forest, oats, rapeseed, spring barley, sunflower, water and winter wheat. Again, winter wheat and spring barley dominates largely the sample. The overall accuracy was chosen as index to follow the evolution of the accuracy of the classifications.

4. RESULTS AND DISCUSSION

Three products were produced for the 2013 growing season. First, an updated land cover map was produced in September to better represent the cropland area extent. A visual analysis revealed that the pre-seasonal cropland layer is spatially consistent to separate urban areas, forests and water. However, it appears that for some fragmented areas, e.g. small forest patches, the spatial resolution is insufficient. Being deprived of natural vegetation class, the cropland is overestimated. The map was quantitatively assessed by the Pareto boundary method which confirmed these observations (Fig. 4). The Pareto boundary helps to understand whether the accuracy of a low spatial resolution map is given by poor performance of the classification algorithm or by the low resolution of the remotely sensed data which had been classified [20]. The region below the Pareto boundary characterizes the low resolution effect; the distance from the boundary to point defined the omission/commission errors of the product is a function of the algorithm performance. The large commission error observed translates the classification of natural vegetation class. Overall accuracy of the cropland class reached 73%.

Second, a crop group layer distinguishing winter crops and summer crops was produced using time-series from September to March. Accuracy of the crop group layer was assessed and showed a global accuracy of 78%. This level of accuracy is satisfactory considering the timing of this early estimation. For the winter wheat class, one can observe a high omission rate but low commission rate. The level of omission might be explained by the tighten-

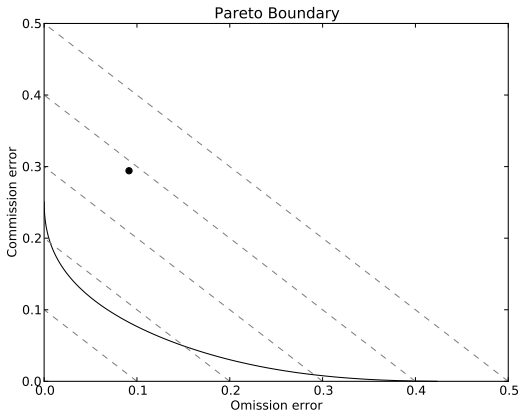

Figure 4. Pareto boundary of the cropland class. MODIS' spatial resolution appears too coarse to capture the fragmented landscapes such as forest patches. The absence of a natural vegetation class introduces commission errors in the cropland class. The dashed lines are the iso-lines of accuracy.

ing of the decision rule. Visual comparison of the product with the time-series and the validation data set showed that the algorithm successfully captured the salient features and omitted those hardly identifiable by human interpretation.

Table 2. Confusion matrix for the Crop Type Layer. The overall accuracy is satisfactory considering the timing of the estimation. The level of omission can be explained by the tightening of the decision rule.

	Reference		
Classification	Other	Winter crops	User Acc.
Other	346	104	0.77
Winter crops	37	143.00	0.79
Producer Acc.	0.90	0.58	
Overall Acc.	0.78		

Third, a crop specific crop layer was produced and updated along the season with Radarsat-2, RapidEye and MODIS images. Quality of the map was assessed following the temporal evolution of the overall accuracy (Fig. 6). Accuracy at the first two acquisitions (+/75%) coincides with the accuracy of the crop group layer (78%). At the third acquisition corresponding to the first RapidEye coverage, accuracy peaks to about 85%. Thus, at the end of May the map meets the accuracy target for crop maps proposed by De Wit and Clevers[9]. From April to August, the overall accuracy follows a ascending trend and reaches 93% at the end of the season. Such behavior might be explained by the dominance of winter wheat and spring barley in the training and validation sample. In a dual situation where two classes dominates

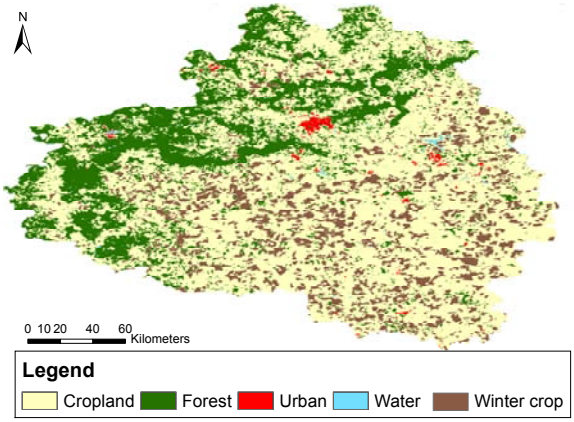

Figure 5. Combination of the pre-seasonal cropland layer and the crop group layer for the year 2013.

and thus influence the mostly the accuracy. Extension of the entire oblast will allow to consider more populated classes and have a more detailed overview.

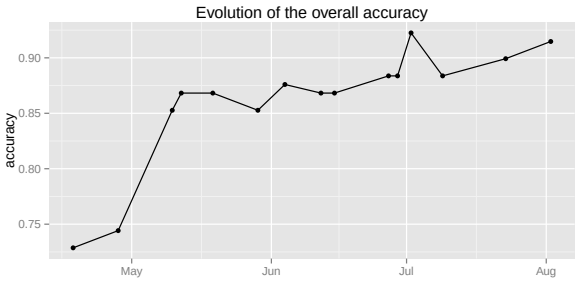

Figure 6. Evolution of the overall accuracy of the crop specific layer along the season. Starting at about 75% percent, the accuracy rapidly reaches 85% (the accuracy target). End-of-season of season accuracy is 93%. The accuracy might be partially explained by the dominance of two constrated classes: winter wheat and spring barley.

5. CONCLUSION

The purpose of this study was to develop a new framework for multi-scale and multi-date crop classification along the growing season to support effective agricultural monitoring. Radarsat-2, RapidEye and MODIS were used as proxies for Sentinel-1, 2 and 3 respectively. The classification system integrates the proxies to produce crop maps updated along the season with an increased number of class and a decreased error rate. This paper presented a three step approach over a large agricultural region in Russia. First, a pre-seasonal cropland layer was derived in August from the previous year time-series thanks to an image-to-map discrepancy approach. Second, a crop group layer that separates winter crops from summer crops was produced in March with an ac-

curacy of 78%. Third, a crop specific map was updated from March to August as images accumulate. Accuracy evolved from 75% to 93% at the end of the season with a large increase in May (85%) corresponding to the first acquisition of RapidEye images. The accuracy figures showed that for agricultural landscapes such as Russia, reliable high resolution crop mask can be derived months before harvest. These promising results still need to be validated at a larger scale.

ACKNOLEDGEMENTS

The above research was carried out as part of the FP-7 IMAGINES[1] project (Implementing Multi-scale AGriculture INdicators Exploiting Sentinels).

REFERENCES

[1] G Genovese, C Vignolles, T Negre, and G Passera. A methodology for a combined use of normalised difference vegetation index and CORINE land cover data for crop yield monitoring and forecasting. A case study on Spain. *Agronomie*, 21(1):91–111, 2001.

[2] C S Murthy, P V Raju, and K V S Badrinath. Classification of wheat crop with multi-temporal images: performance of maximum likelihood and artificial neural networks. *International Journal of Remote Sensing*, 24(23):4871–4890, 2003.

[3] Brian D. Wardlow and Stephen L. Egbert. Large-area crop mapping using time-series MODIS 250 m NDVI data: An assessment for the U.S. Central Great Plains. *Remote Sensing of Environment*, 112(3):1096–1116, March 2008.

[4] Chenghai Yang, James H. Everitt, and Dale Murden. Evaluating high resolution SPOT 5 satellite imagery for crop identification. *Computers and Electronics in Agriculture*, 75(2):347–354, February 2011.

[5] B Deschamps, H McNairn, J Shang, and X Jiao. Towards operational radar-only crop type classification: comparison of a traditional decision tree with a random forest classifier. *Canadian Journal of Remote Sensing*, 38(1):60–68, 2012.

[6] X Blaes, L Vanhalle, and P Defourny. Efficiency of crop identification based on optical and SAR image time series. *Remote Sensing of Environment*, 96(3-4):352–365, 2005.

[7] Prasad S. Thenkabail and Zhuoting Wu. An Automated Cropland Classification Algorithm (ACCA) for Tajikistan by Combining Landsat, MODIS, and Secondary Data. *Remote Sensing*, 4(12):2890–2918, September 2012.

[1] www.http://fp7-imagines.eu/

[8] J Kastens, T Kastens, D Kastens, K Price, E Martinko, and R Lee. Image masking for crop yield forecasting using AVHRR NDVI time series imagery. *Remote Sensing of Environment*, 99(3):341–356, November 2005.

[9] A. J. W. De Wit and J. G. P. W. Clevers. Efficiency and accuracy of per-field classification for operational crop mapping. *International Journal of Remote Sensing*, 25(20):4091–4112, October 2004.

[10] A.B. Potgieter, A. Apan, G. Hammer, and P. Dunn. Early-season crop area estimates for winter crops in NE Australia using MODIS satellite imagery. *ISPRS Journal of Photogrammetry and Remote Sensing*, 65(4):380–387, July 2010.

[11] Heather McNairn, Catherine Champagne, Jiali Shang, Delmar Holmstrom, and Gordon Reichert. Integration of optical and Synthetic Aperture Radar (SAR) imagery for delivering operational annual crop inventories. *ISPRS Journal of Photogrammetry and Remote Sensing*, 64(5):434–449, September 2009.

[12] C. Vancutsem, J.-F. Pekel, P. Bogaert, and P. Defourny. Mean compositing, an alternative strategy for producing temporal syntheses. Concepts and performance assessment for SPOT VEGETATION time series. *International Journal of Remote Sensing*, 28:5123–5141, 2007.

[13] J. Qi, a. Chehbouni, a.R. Huete, Y.H. Kerr, and S. Sorooshian. A modified soil adjusted vegetation index. *Remote Sensing of Environment*, 48(2):119–126, May 1994.

[14] Paul H C Eilers. A Perfect Smoother. *Analytical Chemistry*, 75(14):3631–3636, 2003.

[15] David M. Johnson. A 2010 map estimate of annually tilled cropland within the conterminous United States. *Agricultural Systems*, 114:95–105, January 2013.

[16] Damien Arvor, Milton Jonathan, Margareth Simões Penello, Vincent Dubreuil, and Laurent Durieux. Classification of MODIS EVI time series for crop mapping in the state of Mato. *International Journal of Remote Sensing*, 32(22):7847–7871, 2011.

[17] L Brodsky, L Sourkova, and R Kodesova. Supervised Crop Classification from Middle-resolution Multitemporal Images. In *Proc. of the '2nd MERIS / (A)ATSR User Workshop'*, number 1, pages 1–3, Frascati, Italy, 2008.

[18] Baudouin Desclée, Patrick Bogaert, and Pierre Defourny. Forest change detection by statistical object-based method. *Remote Sensing of Environment*, 102(1-2):1–11, 2006.

[19] Julien Radoux. Updating land cover maps by GIS-driven analysis of very high resolution satellite images. 2010.

[20] L. Boschetti, S. Flasse, and P. Brivio. Analysis of the conflict between omission and commission in low spatial resolution dichotomic thematic products: The Pareto Boundary. *Remote Sensing of Environment*, 91(3-4):280–292, June 2004.

[21] R. Geerken, B. Zaitchik, and J. P. Evans. Classifying rangeland vegetation type and coverage from NDVI time series using Fourier Filtered Cycle Similarity. *International Journal of Remote Sensing*, 26(24):5535–5554, December 2005.

[22] Mark E Jakubauskas, David R Legates, and Jude H Kastens. Crop identification using harmonic analysis of time-series AVHRR NDVI data. *Computers and Electronics in Agriculture*, 37(1-3):127–139, December 2002.

[23] Martin Baatz. Multiresolution Segmentation : an optimization approach for high quality multi-scale image segmentation. *Journal of Photogrammetry and Remote Sensing*, 58(3-4):12–23, 2000.

[24] Leo Breiman. Random Forests. *Machine Learning*, 45(1):5–32, 2001.